



# Regulation of the methanogenesis pathways by hydrogen at transcriptomic level in time

Márk Szuhaj<sup>1</sup> · Balázs Kakuk<sup>1,2</sup> · Roland Wirth<sup>1,3</sup> · Gábor Rákhely<sup>1,4</sup> · Kornél Lajos Kovács<sup>1,3,4</sup> · Zoltán Bagi<sup>1,3,4</sup>

Received: 13 March 2023 / Revised: 22 June 2023 / Accepted: 14 July 2023  
© The Author(s) 2023

## Abstract

The biomethane formation from  $4\text{H}_2 + \text{CO}_2$  by pure cultures of two methanogens, *Methanocaldococcus fervens* and *Methanobacterium thermophilum*, has been studied. The goal of the study was to understand the regulation of the enzymatic steps associated with biomethane biosynthesis by  $\text{H}_2$ , using metagenomic, pan-genomic, and transcriptomic approaches. Methanogenesis in the autotrophic methanogen *M. fervens* could be easily “switched off” and “switched on” by  $\text{H}_2/\text{CO}_2$  within about an hour. In contrast, the heterotrophic methanogen *M. thermophilum* was practically insensitive to the addition of the  $\text{H}_2/\text{CO}_2$  trigger although this methanogen also converted  $\text{H}_2/\text{CO}_2$  to  $\text{CH}_4$ . From practical points of view, the regulatory function of  $\text{H}_2/\text{CO}_2$  suggests that in the power-to-gas (P2G) renewable excess electricity conversion and storage systems, the composition of the biomethane-generating methanogenic community is essential for sustainable operation. In addition to managing the specific hydrogenotrophic methanogenesis biochemistry,  $\text{H}_2/\text{CO}_2$  affected several, apparently unrelated, metabolic pathways. The redox-regulated overall biochemistry and symbiotic relationships in the methanogenic communities should be explored in order to make the P2G technology more efficient.

## Key points

- Hydrogenotrophic methanogens may respond distinctly to  $\text{H}_2/\text{CO}_2$  in bio- $\text{CH}_4$  formation.
- $\text{H}_2/\text{CO}_2$  can also activate metabolic routes, which are apparently unrelated to methanogenesis.
- Sustainable conversion of the fluctuating renewable electricity to bio- $\text{CH}_4$  is an option.

**Keywords** Hydrogenotrophic methanogens · Hydrogen · Methanogenesis · Power to gas · Redox regulation

## Introduction

Anaerobic digestion (AD) is one of the most promising technologies among the renewable and sustainable bioenergy production processes, offering multiple benefits such as waste and by-product biomass utilization, production of

gaseous biofuel, and organic fertilizer (Bagi et al. 2017). Biogenic methane production is a complex microbial process carried out by a unique community of bacteria and archaea. The methanogenic archaea are among the main contributors to the global carbon cycle and exclusively belong to the Euryarchaea phylum (Berghuis et al. 2019). Methanogenesis is an anaerobic respiration process that uses oxidized carbon such as  $\text{CO}_2$  as a terminal electron acceptor (Lyu et al. 2018). The methanogenic archaea are a highly specialized group of microbes as they produce  $\text{CH}_4$ , which is a useful energy carrier when utilized and a powerful greenhouse gas when released. Although methanogens utilize only a limited number of simple substrates, their biochemistry is rather complex and unconventional in the microbial world. Three major pathways of methanogenesis are known: hydrogenotrophic, methylotrophic, and acetoclastic (Conrad 2009; Zhao et al. 2018). The hydrogenotrophic methanogens convert  $\text{H}_2$  and  $\text{CO}_2$  to  $\text{CH}_4$ , and

✉ Zoltán Bagi  
bagiz@brc.hu

<sup>1</sup> Department of Biotechnology, University of Szeged, Szeged, Hungary

<sup>2</sup> Department of Medical Biology, University of Szeged, Szeged, Hungary

<sup>3</sup> Biological Research Center, Institute of Plant Biology, Szeged, Hungary

<sup>4</sup> Biological Research Center, Institute of Biophysics, Szeged, Hungary

the acetoclastic methanogens split acetate to  $\text{CH}_4$  and  $\text{CO}_2$ , while methylotrophic methanogens use methylated compounds for methane production.

Biochemical methane evolution requires at least six unusual coenzymes, some of which are active only at extremely low redox potentials (Lyu et al. 2018). The only enzyme present in all types of methanogenesis is methyl-coenzyme M reductase (Mcr), a Ni-corrinoid protein catalyzing the last step of methyl group reduction to methane (Liu and Whitman 2008). In hydrogenotrophic methanogenesis, the regulatory roles of the local  $\text{H}_2$  levels and interspecies  $\text{H}_2$  transfer have been recognized as a central element in the concerted action of the complex microbial community (Bagi et al. 2007; Giovannini et al. 2016; Sunyoto et al. 2016).  $\text{H}_2$  serves as a delicate safety valve: when  $\text{H}_2$  accumulates, it creates product inhibition of the acetogenic bacteria, which are the main  $\text{H}_2$  producers in the AD community (Ahring and Westermann 1988).

At the same time, hydrogenotrophic methanogens require as much  $\text{H}_2$  as the system can provide, because they use  $\text{H}_2$  for the  $\text{CO}_2$  reduction to  $\text{CH}_4$ . The competition and sustainable equilibrium between  $\text{H}_2$  production by acetogens and  $\text{H}_2$  consumption by hydrogenotrophic methanogens usually result in a very low dissolved  $\text{H}_2$  partial pressure in order to maintain a balanced operation of the entire microbiological community (Vavilin et al. 1995). The extremely low solubility of  $\text{H}_2$  in the aqueous environment is a rate-limiting factor. Consequently, the hydrogenotrophic methanogens starve for  $\text{H}_2$  in the AD processes, and thus, the  $\text{H}_2$  production represents a bottleneck in the biomethane formation (Demirel and Scherer 2008; Kern et al. 2016; Szuhaj et al. 2016).

We demonstrated earlier that reduced accessibility is a regulating element in biogas production and corroborated that the introduction of  $\text{H}_2$ -producing bacteria into a natural biogas-generating consortium appreciably increased the efficacy of biogas production both in batch fermentations and in scaled-up anaerobic digestion (Bagi et al. 2007). The relationship between the acetogens and methanogens is syntrophic, supported by a process called interspecies hydrogen transfer or interspecies electron flow (Rotaru et al. 2014). The actual  $\text{H}_2$  concentration has been shown to determine the composition of the methanogenic community (Ács et al. 2019).

The expression/transcription of genes in hydrogenotrophic methanogens has been reported to change in response to the  $\text{H}_2$  availability, and  $\text{H}_2$  alters the physiology of several microbes belonging to the kingdom Bacteria (Kakuk et al. 2021). Hence, the regulatory role of  $\text{H}_2$  on the expression of methanogenesis genes is instinctively expected.  $\text{H}_2$ -regulated expression of genes, which are apparently not directly involved in  $\text{H}_2$  metabolism, allows the exploration of the underlying metabolic connections and improves our knowledge concerning molecular redox

networks in the biogas-producing microbial community and in environmental microbiology in general.

A rapidly emerging biotechnological application of the  $\text{H}_2$  metabolism of hydrogenotrophic methanogens is the power-to-gas (P2G) system development. This innovative approach employs the ability of hydrogenotrophic methanogens to efficiently reduce  $\text{CO}_2$  using the reducing power of  $\text{H}_2$  generated from renewable electricity via water electrolysis (Szuhaj et al. 2016; De Corato et al. 2022; Pastore et al. 2022). Renewable electricity, produced in a fluctuating manner by the photovoltaic and/or wind energy power plants, can be converted to the easily storable and transportable biomethane energy carrier and introduced into the natural gas pipelines. The benefits and advantages of this energy conversion and storage concept have been discussed recently (Bassani et al. 2016; Angelidaki et al. 2018; Palù et al. 2022). The biological conversion of electrolytically generated reductants to  $\text{CH}_4$  is appealing also as a tool to reduce the carbon footprint imposed upon the Earth by fossil energy-fueled human activities (Yan et al. 2021; Zhang et al. 2022). Biomethanation can be carried out by pure cultures of hydrogenotrophic methanogens or mixed anaerobic microbial communities containing hydrogenotrophic methanogens. The methanogens are more stable in a mixed culture system, and the operational costs are lower, although the molecular events can be followed clearly in pure cultures. The dynamics of the “turn-on” response of the hydrogenotrophic methanogens to the swiftly changing  $\text{H}_2$  supply, which is due to the unpredictable  $\text{H}_2$  generation by the weather-dependent renewable electricity production, is not fully explored yet.

It is astonishing to note the complexity of the molecular machinery, which handles the simplest molecule,  $\text{H}_2$ . The aims of the present study have been to determine the expression levels of the genes involved in hydrogenotrophic methanogenesis and to map the expression profile changes in hydrogenotrophic methanogens during the “turn-on” and “turn-off” phases of P2G conversion.

## Materials and methods

### Strains and media

Strains were obtained from DSMZ (Leibniz Institute DSMZ-German Collection of Microorganisms and Cell Cultures GmbH, Braunschweig). *Methanocaldococcus fervens* (DSM 4213) was isolated from a deep-sea hydrothermal vent sample from Guaymas Basin, Gulf of California (Jeanthon 1999). Growth occurs between 48 and 92 °C, with an optimum of around 85 °C, and between pH 5.5 and 7.6, with an optimum of about pH 6.5. It is a chemolithotrophic strain that uses  $\text{H}_2$  and  $\text{CO}_2$  as energy and carbon

sources to produce methane. *Methanobacterium thermophilum* (DSM 6529) grows between 40 and 70 °C, with an optimum at 55 °C. *M. thermophilum* reduces CO<sub>2</sub> with H<sub>2</sub> but also requires formate and/or acetate for growth (Kotelnikova et al. 1993).

*M. fervens* and *M. thermophilum* were incubated in DSM 282 medium, which initially consisted of 0.14 g L<sup>-1</sup> K<sub>2</sub>HPO<sub>4</sub>; 0.14 g L<sup>-1</sup> CaCl<sub>2</sub> × 2 H<sub>2</sub>O; 0.25 g L<sup>-1</sup> NH<sub>4</sub>Cl; 3.4 g L<sup>-1</sup> MgSO<sub>4</sub> × 7 H<sub>2</sub>O; 4.1 g L<sup>-1</sup> MgCl<sub>2</sub> × 6 H<sub>2</sub>O; 0.33 g L<sup>-1</sup> KCl; 0.5% (v v<sup>-1</sup>) NiCl<sub>2</sub> × 6 H<sub>2</sub>O solution (0.1% w v<sup>-1</sup>); 30 g L<sup>-1</sup> NaCl; 0.1 g L<sup>-1</sup> Fe(NH<sub>4</sub>)<sub>2</sub>(SO<sub>4</sub>)<sub>2</sub> × 6 H<sub>2</sub>O; trace element solution (DSM 141); 0.5% v v<sup>-1</sup> Na-resazurin solution (0.1% w v<sup>-1</sup>); 1 g L<sup>-1</sup> NaHCO<sub>3</sub>; 1% v v<sup>-1</sup> vitamin solution (DSM 141); 0.5 g L<sup>-1</sup> L-cysteine-HCl × H<sub>2</sub>O; and 0.5 g L<sup>-1</sup> Na<sub>2</sub>S × 9 H<sub>2</sub>O. The trace element solution (DSM 141) contained 2 g L<sup>-1</sup> biotin; 2 g L<sup>-1</sup> folic acid; 10 g L<sup>-1</sup> pyridoxine hydrochloride; 5 g L<sup>-1</sup> thiamine hydrochloride; 5 g L<sup>-1</sup> riboflavin hydrochloride; 5.0 g L<sup>-1</sup> nicotinic acid; 5 g L<sup>-1</sup> DL-calcium pantothenate; 0.1 g L<sup>-1</sup> vitamin B12; 5 g L<sup>-1</sup> *p*-aminobenzoic acid; and 5 g L<sup>-1</sup> lipoic acid. The vitamin solution (DSM 141) contained 1.5 g L<sup>-1</sup> nitrilotriacetic acid; 3 g L<sup>-1</sup> MgSO<sub>4</sub> × 7 H<sub>2</sub>O; 0.5 g L<sup>-1</sup> MnSO<sub>4</sub> × H<sub>2</sub>O; 1 g L<sup>-1</sup> NaCl; 0.1 g L<sup>-1</sup> FeSO<sub>4</sub> × 7 H<sub>2</sub>O; 0.18 g L<sup>-1</sup> CoSO<sub>4</sub> × 7 H<sub>2</sub>O; 0.1 g L<sup>-1</sup> CaCl<sub>2</sub> × 2 H<sub>2</sub>O; 0.18 g L<sup>-1</sup> ZnSO<sub>4</sub> × 7 H<sub>2</sub>O; 0.01 g L<sup>-1</sup> CuSO<sub>4</sub> × 5 H<sub>2</sub>O; 0.02 g L<sup>-1</sup> KAl(SO<sub>4</sub>)<sub>2</sub> × 12 H<sub>2</sub>O; 0.01 g L<sup>-1</sup> H<sub>3</sub>BO<sub>3</sub>; 0.01 g L<sup>-1</sup> Na<sub>2</sub>MoO<sub>4</sub> × 2 H<sub>2</sub>O; 0.03 g L<sup>-1</sup> NiCl<sub>2</sub> × 6 H<sub>2</sub>O; 0.3 mg L<sup>-1</sup> Na<sub>2</sub>SeO<sub>3</sub> × 5 H<sub>2</sub>O; and 0.3 mg L<sup>-1</sup> Na<sub>2</sub>WO<sub>4</sub> × 2 H<sub>2</sub>O. The pH of the completed medium was adjusted to 7–7.2. The headspaces of the reactors were replaced by a sterile 80% H<sub>2</sub> and 20% CO<sub>2</sub> gas mixture. The pure cultures have been maintained in anaerobic serum bottles.

### Fermentation system

The reaction vessels simulate a CSTR (continuous-stirred tank reactor) system, using Braun CT5-2 (B. Braun Biotech International GmbH., Melsungen, Germany) bioreactors with a total volume of 5 L and 2 L of headspace. The sterile media were inoculated with methanogen cultures in 1 V/V%. The sealed headspaces of the reactors were replaced by flushing with a sterile gas mixture of 80% H<sub>2</sub> and 20% CO<sub>2</sub> from a gas cylinder (Linde, Dublin, Ireland; 5 min, 2.5 L min<sup>-1</sup>). The incubation temperature of the reactors was 55 °C (*M. thermophilum*) and 85 °C (*M. fervens*), respectively. Methanogens were cultivated until OD<sub>600nm</sub> = 0.15–0.20. In the case of *M. fervens*, it required 1 day, and in the case of *M. thermophilum*, 4 days were needed to achieve this cell density. When the expected optical density was reached, the first samples (150 mL) were taken for transcriptomic analysis, and these were marked as Metfer\_H<sub>2</sub>\_start and Metthe\_H<sub>2</sub>\_start, respectively (see figures). The headspace was then replaced with sterile N<sub>2</sub>

(Linde 4.5, 5 min, 2.5 L min<sup>-1</sup>) for 1 h, and these samples were entitled Metfer\_N<sub>2</sub>. In order to examine the response of the heterotrophic *M. thermophilum* to the withdrawal of H<sub>2</sub>/CO<sub>2</sub>, Na-acetate (1 g L<sup>-1</sup>) and Na-formate (3 g L<sup>-1</sup>) were injected into the corresponding reactors. Metthe\_N<sub>2</sub> + VFA sampling took place after 1 h following the H<sub>2</sub> supply “turn-off” event. Afterward, the headspaces of the reactors were readjusted to H<sub>2</sub>/CO<sub>2</sub> (Linde, 5 min, 2.5 L min<sup>-1</sup>). The last samples were taken after an additional 1-h incubation, these were labeled “Metfer\_H<sub>2</sub>\_end” and “Metthe\_H<sub>2</sub> + VFA\_end.” The whole procedure was repeated three times, and the transcriptomic analysis processed the data of three biological parallels. Samples taken from the three parallel experiments were pooled for RNA isolation and sequencing.

### Total RNA isolation and transcriptome sequencing

The RNA extractions were carried out with the Zymo Research Soil/Fecal RNA kit (R2040, Zymo Research, Irvine, CA, USA). After lysis (bead beating), the Zymo Research kit protocol was followed. The DNA contamination was removed by Thermo Scientific Rapid Out™ DNA removal kit (K2981, Thermo Fisher Scientific, Waltham, MA, USA). Before transcriptome sequencing, rRNA was depleted from RNA by using the Gram +/Gram – depletion kit in a 60:40 ratio (RiboMinus A15020 Life Technologies, San Francisco, CA, USA). The mRNA library was prepared using the mRNA Sample Prep kit (Illumina, San Diego, CA, USA). Sequencing was performed using the Illumina V2 chemistry (2 × 250 bp) and applying the MiSeq paired-end mode. Raw sequences are available on the NCBI Sequence Read Archive (SRA) under the accession number: PRJNA922065.

### Pangenome construction and mapping of transcript data on gene clusters

The genome of *M. thermophilum* and *M. fervens* was downloaded from the NCBI Genome database. The Anvi’o (v7 “Hope”) (Eren et al. 2015) pan-genomics workflow was used in computing the archaeal pangenome. In the first step, genome databases were generated where DNA and amino acid sequences, functional annotations (based on InterPro and COG (clusters of orthology groups of proteins) databases), and databases of each gene in genomes were stored. In the second step, pangenome was built up in the following way: (1) calculation of amino acid similarities between the genomes using blastp, (2) identification of gene clusters with MCL (Markov Cluster) algorithm, (3) computation of a total number of genes, gene clusters across genomes, and core clusters that appear in both genomes, and (4) hierarchical clustering analysis for gene clusters and genomes using the Euclidean distance and the Ward clustering. In this step,

transcriptomic data were used to create a “pan-genomics” analysis based on (Delmont and Eren 2018) where the average coverage of genes in gene clusters across genomes was recovered. In the final step, pangenome was visualized by Anvi'o interactive interface. For measuring the change in the expression level of genes ( $\log_2$  fold change), CLC Genomics Workbench (v20) was employed ( $\log_2$  fold change calculation).

## Results

*M. fervens*, being an obligate hydrogenotrophic methanogen, showed active expression of the core and the accessory genes (Fig. 1: Metfer\_H<sub>2</sub>\_start) in the H<sub>2</sub>/CO<sub>2</sub>-rich environment. The core genes, which are directly involved in hydrogenotrophic methanogenesis, were highly expressed upon supplying H<sub>2</sub>/CO<sub>2</sub>, relative to the accessory genes (see the blue line marked “core” in Fig. 1). When the headspaces of the

reactors were replaced by N<sub>2</sub> for 1 h, the expression profiles changed relative to the H<sub>2</sub>/CO<sub>2</sub> that supported hydrogenotrophic metabolism (Fig. 1 Metfer\_N<sub>2</sub>). Upon replacing the gas phase again with the initial H<sub>2</sub>/CO<sub>2</sub>, the transcriptomic activity of *M. fervens* was recovered (Metfer\_H<sub>2</sub>\_end). The expression of the genes after 1 h reached almost the starting level.

It is noteworthy, that the genome-wide transcript profile clearly indicated the negative effect of the H<sub>2</sub>/CO<sub>2</sub> withdrawal on the expressions of the core methanogenesis and the accessory genes in *M. fervens*. The most pronounced changes were apparent among the methanogenesis-related genes (Fig. 2). Some of these genes code for methanogenesis marker proteins, such as those playing an important role in the functional activity of the hydrogenotrophic methane formation, i.e., methylene-tetrahydromethanopterin (methylene-H<sub>4</sub>MPT) reductase, -hydrogenase, coenzyme F<sub>420</sub> reducing hydrogenase, F<sub>420</sub> hydrogenase, CoB-CoM heterodisulfide reductase, F<sub>420</sub>-dependent methylene-H<sub>4</sub>MPT

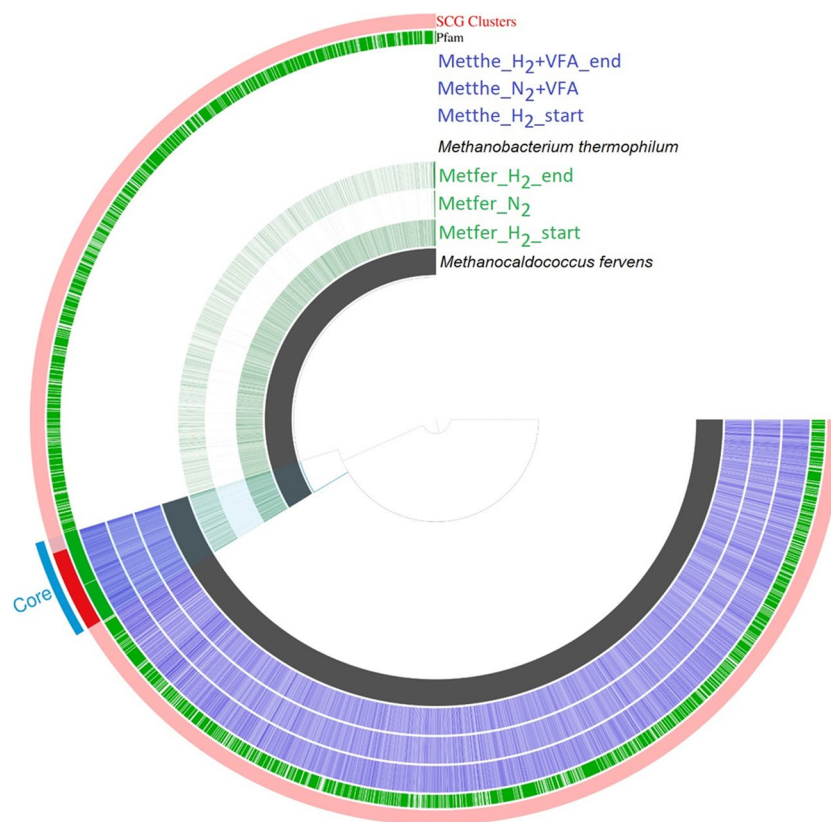


**Fig. 1** The pangenome and metatranscriptome of *M. fervens* (Metfer) and *M. thermophilum* (Metthe). The innermost ring shows the total genome of *M. fervens* (black). The next 3 layers represent the coverage of the genes which were annotated in the genome (the color darkness increases with the gene coverages) at the 3 sampling points: Metfer\_H<sub>2</sub>\_start, Metfer\_N<sub>2</sub>, and Metfer\_H<sub>2</sub>\_end. The 4th ring represents the total genome of *M. thermophilum* (black). The next 3 layers represent the coverage of the genes which were annotated in the

genome (the color darkness increases with the gene coverages) at the 3 sampling points: Metthe\_H<sub>2</sub>\_start, Metthe\_N<sub>2</sub>+VFA, and Metthe\_H<sub>2</sub>+VFA\_end. The green ring indicates the gene clusters in which at least one gene was functionally annotated using Pfams. In the outermost ring, the red bands represent the distribution of SCG clusters (genes, that are present in both organisms and overlap) of the two archaea. The blue band marks the position of core hydrogenotrophic methanogenesis genes in the two genomes

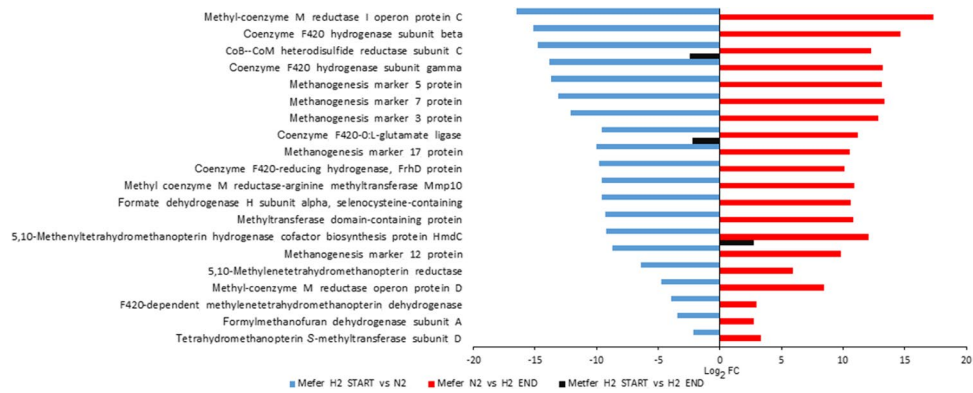


**Fig. 2** Significant ( $-2 \geq \log_2 FC \geq 2$ ) gene expression changes in the core transcriptome of *M. fervens* (Metfer). Blue bars: expression changes between H<sub>2</sub>/CO<sub>2</sub> versus N<sub>2</sub> supplied (Metfer\_H<sub>2</sub>\_start and Metfer\_N<sub>2</sub> samples). Red bars: expression changes between Metfer\_N<sub>2</sub> and Metfer\_H<sub>2</sub>\_

end samples. Black bars: expression changes between Metfer\_H<sub>2</sub>\_start and Metfer\_H<sub>2</sub>\_end samples.  $\log_2 FC = \log_2 \left( \frac{\text{relative abundance sample 1}}{\text{relative abundance sample 2}} \right)$

dehydrogenase, formate dehydrogenase, formylmethanofuran dehydrogenase, methyl-coenzyme M reductase, and tetrahydromethanopterin S-methyltransferase. Correlation between the scale of alteration in the biological activity of several genes in response to H<sub>2</sub>/CO<sub>2</sub> “switch on” and “switch off” could be observed, see blue and red horizontal columns in Fig. 2. The restoration of the methanogenic activity at the transcriptomic level corroborates rapid H<sub>2</sub>-driven response, which is shorter than 1 h in this system, in the obligate autotrophic *M. fervens* (Figs. 1 and 2).

The metabolism of *M. thermophilum* differs from that of *M. fervens*. *M. thermophilum* is also a hydrogenotrophic archaeon able to utilize H<sub>2</sub> for CO<sub>2</sub> reduction but needs formate/acetate (volatile fatty acids (VFA)) in its heterotrophic lifestyle (Rivard and Smith 1982; Maestrojuan et al. 1990). The injected VFA sustained the apparent biological activity of the core and accessory genes. Thus, significant changes did not appear upon “H<sub>2</sub> starvation.” VFA, the alternative methanogenesis substrate, compensated for the H<sub>2</sub> absence in the hydrogenotrophic metabolism; therefore, the

methanogenesis-related genes remained highly expressed (Fig. 1). Nevertheless, the detailed analysis of the core gene expressions revealed significant transcriptional changes (Fig. 3).

It is noted at first glance that differential expression and biological activity of the hydrogenotrophic methanogenesis genes were not evident in *M. thermophilum*. Heterotrophic methanogenesis took over after the withdrawal of the H<sub>2</sub>/CO<sub>2</sub> supply; hence, the methanogenesis-related genes were still expressed and ready to perform the expected biological activity. That is why in the differential expression profiles the genes coding for key enzymes of hydrogenotrophic metabolism did not emerge (Fig. 3). The removal of the H<sub>2</sub>/CO<sub>2</sub> and concomitant addition of VFA increased the expression of a nucleotide-binding protein and the S-adenosylmethionine decarboxylase. S-Adenosylmethionine decarboxylase is a polyamine that functions as an activated methyl donor for cells to modify RNA, DNA, proteins, lipids, and cofactors and has an alternate function in spermidine biosynthesis (Kim

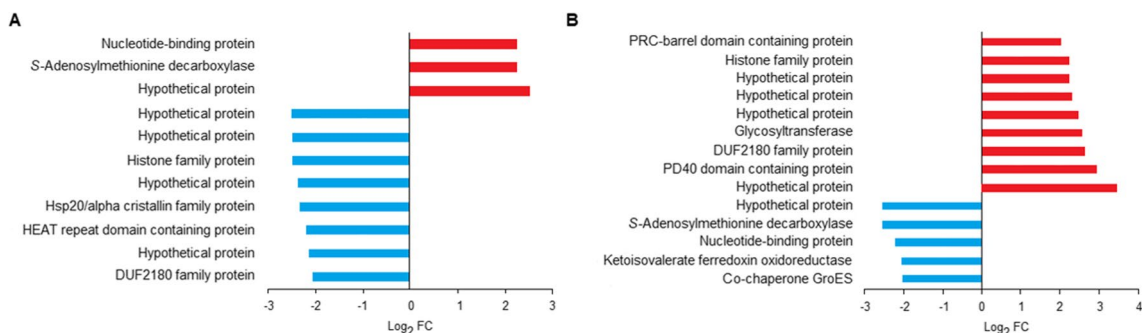


**Fig. 3** Significant ( $-2 \geq \log_2 FC \geq 2$ ) gene expression changes in the core transcriptome of *M. thermophilum* (Metthe). **A** Negative (blue bars) and positive (red bars) expression changes between Metthe\_H<sub>2</sub>\_start and

Metthe\_N<sub>2</sub>+VFA samples. **B** Negative (blue bars) and positive (red bars) expression changes between Metthe\_N<sub>2</sub>+VFA and Metthe\_H<sub>2</sub>+VFA\_end samples.  $\log_2 FC = \log_2 \left( \frac{\text{relative abundance sample 1}}{\text{relative abundance sample 2}} \right)$

et al. 2000). The change of the gas supply significantly decreased the expression of several hypothetical proteins, such as the domain of unknown function (DUF) 2180 protein, histone family protein, heat repeat domain-containing protein, and Hsp20/alpha crystallin family protein. Most of these genes code for proteins of unknown or poorly understood functions. Heat shock proteins take part in the protection against environmental stresses. They act as chaperons, protecting target proteins from denaturation, aggregation, and inactivation. Reversing the supply of  $H_2/CO_2$  elevated the expression of the genes coding for unknown proteins, protein domains (hypothetical proteins, DUF 2180 protein, PD40 domain-containing protein, PRC-barrel domain-containing protein, histone family protein, and glycosyltransferase. The transient elevated partial pressure of  $H_2/CO_2$  inhibited the expression of ketoisovalerate ferredoxin oxidoreductase and *S*-adenosylmethionine decarboxylase. Ketoisovalerate ferredoxin oxidoreductase catalyzes the coenzyme A-dependent oxidation of branched-chain 2-ketoacids coupled to the reduction of ferredoxin (Heider et al. 1996).

The investigation of the mRNA-predicted COGs (clusters of orthology groups of proteins) helps to track the changes of functionally connected gene groups. The COG analysis correlated with the expression profiles of the whole genome (Fig. 1).

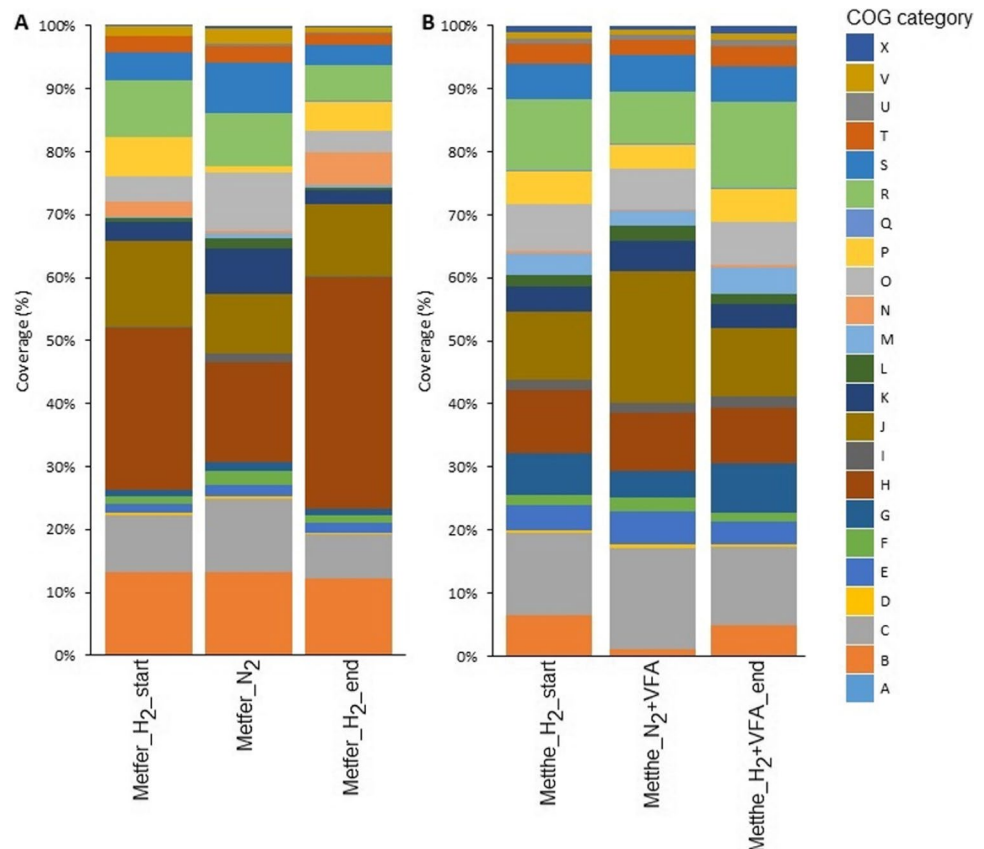
Despite the distinct fermentation environments, the COGs' changes were similar in both organisms (Fig. 4).

The most spectacular change was the decrease in the expression of category H genes in response to  $H_2/CO_2$  removal in *M. fervens*. The coenzyme transport and metabolism genes (COG H) expressed the majority of the annotated sequences under  $H_2/CO_2$  (25.66% in Metfer\_  $H_2$ \_start) in *M. fervens*, which decreased to 15.98% upon diminishing  $H_2/CO_2$ . (Metfer\_  $N_2$ ) After restoring  $H_2/CO_2$  feeding, the expression of the COG group H genes was quickly reactivated, and the gene activity of the COG group H surpassed the previously detected level (36.64%, Metfer\_  $H_2$ \_end).

The transcriptomic changes of the genes coding for coenzyme transport and metabolism (COG H) group were less dominant in *M. thermophilum* during similar treatment. These genes were similarly abundant (10.08%) as those belonging in category C (energy production and conversion, 13.14%), K (transcription, 10.85%), and R (predicted general functions, 11.22) COGs. Following the  $H_2$  gas supply switch-off, no remarkable changes were detected presumably due to the activation of the heterotrophic methanogenic pathway via the organic substrate addition. Restoring the  $H_2/CO_2$  supply did not increase the transcriptomic activity of the genes in these categories.

COG category C harbors most of the core genes of hydrogenotrophic methanogenesis. As opposed to the H

**Fig. 4** Transcriptomic changes in the COG categories due to the presence and absence of reductants ( $H_2$  or  $H_2 + VFA$ ) in *M. fervens* (Metfer) and *M. thermophilum* (Metthe), respectively. The coverage % values represent the coverage of the COGs relative to the total genes annotated in the genomes



category, expression of genes in category C remained stable throughout the entire fermentation, the H<sub>2</sub>/CO<sub>2</sub> withdrawal slightly elevated the relative read coverage of these genes from 9.03 to 11.56% in *M. fervens* and from 13.14 to 16.13% in *M. thermophilum*, respectively. Surprisingly, COG category J genes showed high expression upon H<sub>2</sub>/CO<sub>2</sub> withdrawal in *M. thermophilum*, which might be due to the obligatory addition of VFA to sustain *M. thermophilum*, rather than displaying an effect of changing gas phase composition. Category J genes code for translation, ribosomal structure, and biogenesis; hence, they may not be directly linked with hydrogenotrophic methanogenesis.

No hydrogenotrophic methanogenesis-related significant ( $-2 \geq \log_2 FC \geq 2$ ) COG changes occurred in *M. fervens* in I (lipid transport and metabolism), N (cell motility), P (inorganic ion transport and metabolism), U (intracellular trafficking, secretion, and vesicular transport), and X (nuclear structure) and in *M. thermophilum* in B (chromatin structure and dynamics). These COGs are therefore not directly connected with the hydrogenotrophic metabolism in these Archaea.

## Discussion

Our aim in this study was to determine the transcriptional activity of two thermophilic hydrogenotrophic methanogens (*M. fervens*, *M. thermophilum*) in response to H<sub>2</sub>/CO<sub>2</sub> “turn-on” and “turn-off” conditions. The two strains utilize somewhat distinct methanogenesis pathways in the presence of various carbon sources (Ferry 2011). H<sub>2</sub> is oxidized, and CO<sub>2</sub> is reduced to CH<sub>4</sub> in the obligate auxotrophic hydrogenotrophic CO<sub>2</sub>-reduction pathway, e.g., in *M. fervens* (Jeanthon 1999). Both strains are able to reduce CO<sub>2</sub> via the auxotrophic pathway, but *M. thermophilum* also requires formate and/or acetate for growth and operates according to facultative hydrogenotrophic methanogenesis (Narihiro et al. 2016).

Pan-genomics-based transcriptomics provides detailed information about core and accessory genes in closely related genomes (Delmont and Eren 2018). The results uncover the transcriptomic activity of specific strains, which tell us how actively the functions of the particular genes, or clusters thereof, have worked at the time of sampling. The H<sub>2</sub>/CO<sub>2</sub> removal by replacing the dissolved gases with inert N<sub>2</sub> gas predestined a shift in the hydrogenotrophic gene expression and the alteration of the methanogenic metabolism in both studied hydrogenotrophic organisms. The questions were as follows: which genes were turned on and off upon this intervention and what was the time duration needed for changing the on–off switch position? What were the conceivable effects of the observed pan-genomic/

pan-transcriptomic changes from the point of view of an operating P2G system?

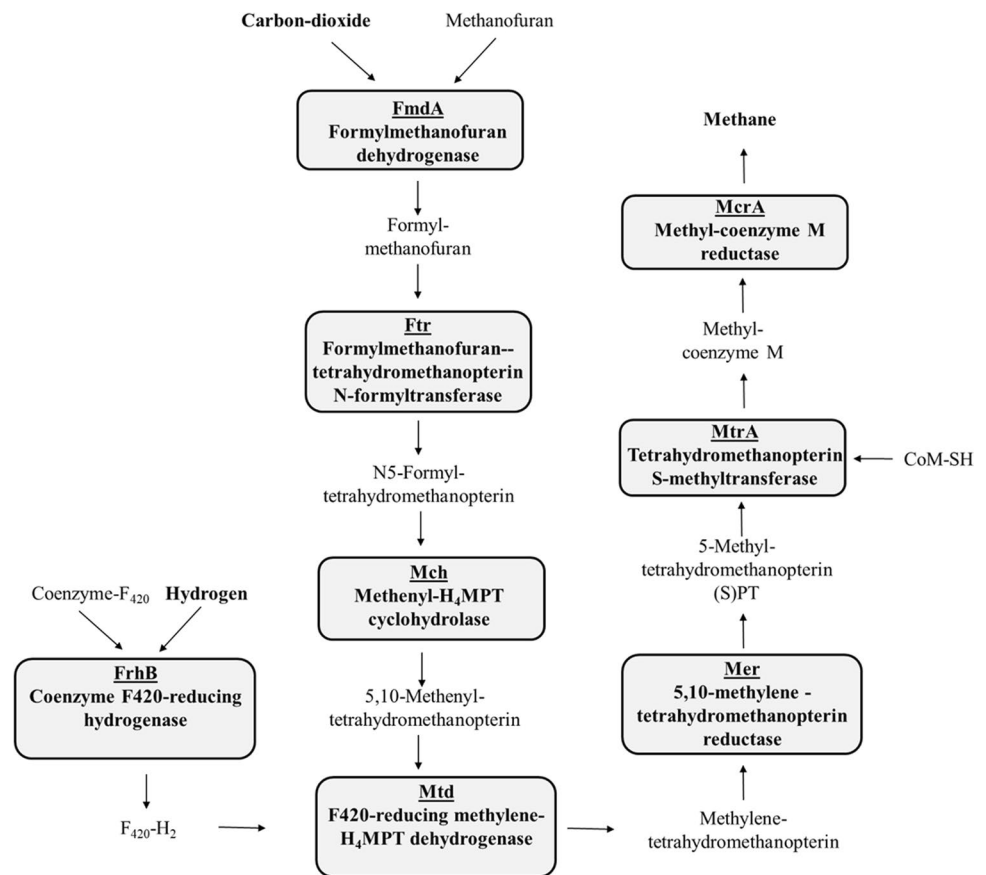
A fundamental difference in gene expression profiles between obligate autotrophic (*M. fervens*) and facultative heterotrophic (*M. thermophilum*) methanogenesis was displayed (Fig. 1). Taking this difference into account, the same experimental protocol was applied for both strains. The total transcript changes indicated rapid inhibition of obligate autotrophic methanogenesis in *M. fervens* upon the diminishing H<sub>2</sub>/CO<sub>2</sub> supply. The majority of the genes in the genome were apparently also affected, indicating a general reorganization of the genome expression profile. *M. fervens* was able to rapidly restore its expressional activity after replenishing H<sub>2</sub>/CO<sub>2</sub>. This observation is interpreted as a relatively quick reorganization of interconnected and apparently unrelated gene expression networks. In contrast, the hydrogenotrophic methanogenesis in *M. thermophilum* did not go through similar remarkable gene expression change. The available organic VFA kept the hydrogenotrophic gene expression at a stable level in the absence of H<sub>2</sub>/CO<sub>2</sub>. In the power-to-gas applications, *M. fervens* would be more suitable than *M. thermophilum*, although using the mixed anaerobic methanogen communities for the P2G operation seems the best choice based on economical considerations and operational stability.

This study also demonstrated that almost the entire metabolism of hydrogenotrophic methanogens is affected by the presence or absence of H<sub>2</sub>/CO<sub>2</sub>. The present knowledge does not allow drawing any specific conclusion about the contribution of the hitherto largely unknown metabolic pathways to the hydrogenotrophic methanogenesis. Nevertheless, these observations demand further systematic studies. The distant metabolic routes are presumably coupled to the intracellular redox regulation in hydrogenotrophic archaea.

Among the COG categories, the genes belonging to categories C and H deserve special attention. The genes in the COG category C are responsible for energy production and conversion (Tatusov et al. 2001), and together with the genes in the COG category H, they are the most highly expressed groups in methanogens (Gilmore et al. 2017). Formylmethanofuran dehydrogenase, coenzyme F<sub>420</sub>-reducing hydrogenase/dehydrogenase, and F<sub>420</sub>-dependent methylene-tetrahydromethanopterin dehydrogenase (Mtd) core hydrogenotrophic methanogenic genes of COG category C were annotated in the two archaea.

Formylmethanofuran dehydrogenase is the first enzyme of the hydrogenotrophic methanogenesis pathway. This enzyme catalyzes the binding of CO<sub>2</sub> to the amino group of methanofuran, forming formylmethanofuran (Bertram et al. 1994). Coenzyme F<sub>420</sub>-reducing hydrogenase is responsible for the formation of reduced coenzyme F<sub>420</sub> (F<sub>420</sub>H<sub>2</sub>), which is the electron donor for the methenyl-tetrahydromethanopterin (methenyl-H<sub>4</sub>MPT) reduction. Additionally, the F<sub>420</sub>H<sub>2</sub>

**Fig. 5** Schematic diagram of the hydrogenotrophic methanogenesis pathway



is one of the electron sources for the  $F_{420}$   $H_2$ -dependent methylene-tetrahydromethanopterin dehydrogenase (Mtd) (Hendrickson and Leigh 2008). Tetrahydromethanopterin *S*-methyltransferase (Mtr) is a membrane-associated enzyme complex, which catalyzes a  $Na^+$  translocation-dependent methyl transfer from methyl-tetrahydromethanopterin (methyl- $H_4$ MPT) to coenzyme M (CoM-SH), creating methyl-coenzyme M ( $CH_3$ -S-CoM). Methyl-coenzyme M ( $CH_3$ -S-CoM) is a precursor molecule of the heterodisulfide complex (CoB-S-S-CoM) formation. Methyl-coenzyme M reductase (Mcr) catalyzes the reduction of methyl-coenzyme M ( $CH_3$ -S-CoM) with coenzyme B (CoB-SH) (Wagner et al. 2018) Fig. 5.

The genes of the H category regulate coenzyme transport and metabolism, so they code for methanogenesis (methyl-coenzyme M reductase (mcr)) (Thauer 1998) and the hydrogenotrophic methanogenesis-related enzyme (tetrahydromethanopterin *S*-methyltransferase (mtr)) (Wagner et al. 2018).

Previous studies demonstrated that gene expression levels in *Bacteria* reached the maximum in most cases within 1 h (Golding et al. 2005). We found in mixed enriched hydrogenotrophic cultures a similar time range (<2–12 h) in the response to  $H_2/CO_2$  addition at mesophilic conditions (Szuhaj et al. 2016; Kakuk et al. 2021) limited by the

solubility of  $H_2$  in the aqueous system. In line with these observations, in the present study, the absence of  $H_2/CO_2$  resulted in fading gene expression along the whole genome of the *M. fervens* (domain Archaea) in less than 1 h, which is only an upper time limit we could reach in this system. This is an important message for practical power-to-gas renewable electricity conversion and storage systems as in real-life P2G operation, and the biological component is not a rate-limiting component in most cases. The results thus confirm that hydrogenotrophic methanogens are effective, flexible, and easily manageable biological agents to convert the intermittently produced renewable electricity, generated by photovoltaics and/or wind power, to storable and transportable biomethane. In addition, we know from earlier studies (Szuhaj et al. 2016) that the microbial community can hibernate and inactivate itself for an extended period of time when not needed to perform. Taken together, these observations offer additional possibilities for the development of optimized microbiological communities for the P2G industry.

**Acknowledgements** This study has been supported in part by the Hungarian National Research, Development and Innovation Fund project 2020-3.1.2-ZFR-KVG-2020-00009. RW, ZB and KLK received support from the Hungarian NRDIF fund projects, PD132145, K143198, FK123902 and 2019-2.1.13-TÉT\_IN-2020-00016.



**Author contribution** ZB, KLK, and MSZ designed and conducted the experiments and wrote the manuscript. RW and BK performed the bioinformatics analyses. KLK and GR analyzed the data. All authors read and approved the final manuscript.

**Funding** Open access funding provided by University of Szeged. This study has been supported in part by the Hungarian National Research, Development and Innovation Fund project 2020–3.1.2-ZFR-KVG-2020–00009. RW, ZB, and KLK received support from the Hungarian NRDIF fund projects, PD 132145, K143198, FK123902, and 2019–2.1.13-TÉT\_IN-2020–00016.

**Data availability** The raw metagenome and transcriptome sequences generated and analyzed during the current study were deposited in NCBI under the bioproject accession numbers: PRJNA922065.

## Declarations

**Ethics approval** Not relevant.

**Conflict of interest** The authors declare no competing interests.

**Open Access** This article is licensed under a Creative Commons Attribution 4.0 International License, which permits use, sharing, adaptation, distribution and reproduction in any medium or format, as long as you give appropriate credit to the original author(s) and the source, provide a link to the Creative Commons licence, and indicate if changes were made. The images or other third party material in this article are included in the article's Creative Commons licence, unless indicated otherwise in a credit line to the material. If material is not included in the article's Creative Commons licence and your intended use is not permitted by statutory regulation or exceeds the permitted use, you will need to obtain permission directly from the copyright holder. To view a copy of this licence, visit <http://creativecommons.org/licenses/by/4.0/>.

## References

- Ács N, Szuhaj M, Wirth R, Bagi Z, Maróti G, Rákhely G, Kovács KL (2019) Microbial community rearrangements in power-to-biomethane reactors employing mesophilic biogas digestate. *Front Energy Res* 7:1–15. <https://doi.org/10.3389/fenrg.2019.00132>
- Ahring BK, Westermann P (1988) Product inhibition of butyrate metabolism by acetate and hydrogen in a thermophilic coculture. *Appl Environ Microbiol* 54:2393–2397. <https://doi.org/10.1128/aem.54.10.2393-2397.1988>
- Angelidaki I, Treu L, Tsapekos P, Luo G, Campanaro S, Wenzel H, Kougias PG (2018) Biogas upgrading and utilization: current status and perspectives. *Biotechnol Adv* 36:452–466. <https://doi.org/10.1016/j.biotechadv.2018.01.011>
- Bagi Z, Ács N, Bálint B, Horváth L, Dobó K, Perei KR, Rákhely G, Kovács KL (2007) Biotechnological intensification of biogas production. *Appl Microbiol Biotechnol* 76:473–482. <https://doi.org/10.1007/s00253-007-1009-6>
- Bagi Z, Ács N, Böjti T, Kakuk B, Rákhely G, Strang O, Szuhaj M, Wirth R, Kovács KL (2017) Biomethane: the energy storage, platform chemical and greenhouse gas mitigation target. *Anaerobe* 46:13–22. <https://doi.org/10.1016/j.anaerobe.2017.03.001>
- Bassani I, Kougias PG, Angelidaki I (2016) In-situ biogas upgrading in thermophilic granular UASB reactor: key factors affecting the hydrogen mass transfer rate. *Bioresour Technol* 221:485–491. <https://doi.org/10.1016/j.biortech.2016.09.083>
- Berghuis BA, Yu FB, Schulz F, Blainey PC, Woyke T, Quake SR (2019) Hydrogenotrophic methanogenesis in archaeal phylum *Verstraetearchaeota* reveals the shared ancestry of all methanogens. *Proc Natl Acad Sci U S A* 116:5037–5044. <https://doi.org/10.1073/pnas.1815631116>
- Bertram PA, Karrasch M, Schmitz RA, Böcher R, Albracht SPI, Thauer RK (1994) Formylmethanofuran dehydrogenases from methanogenic archaea substrate specificity, EPR properties and reversible inactivation by cyanide of the molybdenum or tungsten iron-sulfur proteins. *Eur J Biochem* 220:477–484. <https://doi.org/10.1111/j.1432-1033.1994.tb18646.x>
- Conrad R (2009) The global methane cycle: recent advances in understanding the microbial processes involved. *Environ Microbiol Rep* 1:285–292. <https://doi.org/10.1111/j.1758-2229.2009.00038.x>
- De Corato A, Saedi I, Riaz S, Mancarella P (2022) Aggregated flexibility from multiple power-to-gas units in integrated electricity-gas-hydrogen distribution systems. *Electr Power Syst Res* 212:108409. <https://doi.org/10.1016/j.epsr.2022.108409>
- Delmont TO, Eren AM (2018) Linking pangenomes and metagenomes: the *Prochlorococcus* metapangenome. *PeerJ* 6:e4320. <https://doi.org/10.7717/peerj.4320>
- Demirel B, Scherer P (2008) The roles of acetotrophic and hydrogenotrophic methanogens during anaerobic conversion of biomass to methane: a review. *Rev Environ Sci Biotechnol* 7:173–190. <https://doi.org/10.1007/s11157-008-9131-1>
- Eren AM, Esen ÖC, Quince C, Vineis JH, Morrison HG, Sogin ML, Delmont TO (2015) Anvi'o: an advanced analysis and visualization platform for 'omics data. *PeerJ* 3:e1319. <https://doi.org/10.7717/peerj.1319>
- Ferry JG (2011) Fundamentals of methanogenic pathways that are key to the biomethanation of complex biomass. *Curr Opin Biotechnol* 22:351–357. <https://doi.org/10.1016/j.copbio.2011.04.011>
- Gilmore SP, Henske JK, Sexton JA, Solomon KV, Seppälä S, Yoo JI, Huyett LM, Pressman A, Cogan JZ, Kivenson V, Peng X, Tan YP, Valentine DL, O'Malley MA (2017) Genomic analysis of methanogenic archaea reveals a shift towards energy conservation. *BMC Genomics* 18:1–14. <https://doi.org/10.1186/s12864-017-4036-4>
- Giovannini G, Donoso-Bravo A, Jeison D, Chamy R, Ruíz-Filippi G, Vande Wouwer A (2016) A review of the role of hydrogen in past and current modelling approaches to anaerobic digestion processes. *Int J Hydrogen Energy* 41:17713–17722. <https://doi.org/10.1016/j.ijhydene.2016.07.012>
- Golding I, Paulsson J, Zawilski SM, Cox EC (2005) Real-time kinetics of gene activity in individual bacteria. *Cell* 123:1025–1036. <https://doi.org/10.1016/j.cell.2005.09.031>
- Heider J, Mai X, Adams MW (1996) Characterization of 2-ketoisovalerate ferredoxin oxidoreductase, a new and reversible coenzyme A-dependent enzyme involved in peptide fermentation by hyperthermophilic archaea. *J Bacteriol* 178:780–787. <https://doi.org/10.1128/jb.178.3.780-787.1996>
- Hendrickson EL, Leigh JA (2008) Roles of coenzyme F420-reducing hydrogenases and hydrogen- and F420-dependent methylene-tetrahydromethanopterin dehydrogenases in reduction of F420 and production of hydrogen during methanogenesis. *J Bacteriol* 190:4818–4821. <https://doi.org/10.1128/JB.00255-08>
- Jeanthon C (1999) *Methanococcus vulcanius* sp. nov., a novel hyperthermophilic methanogen isolated from East Pacific Rise, and identification of *Methanococcus* sp. DSM 4213T as *Methanococcus fervens* sp. nov. *Int J Syst Bacteriol* 583–589
- Kakuk B, Wirth R, Maróti G, Szuhaj M, Rákhely G, Laczi K, Kovács KL, Bagi Z (2021) Early response of methanogenic archaea to H<sub>2</sub> as evaluated by metagenomics and metatranscriptomics. *Microb Cell Fact* 20:1–18. <https://doi.org/10.1186/s12934-021-01618-y>
- Kern T, Theiss J, Röske K, Rother M (2016) Assessment of hydrogen metabolism in commercial anaerobic digesters. *Appl Microbiol Biotechnol* 100:4699–4710. <https://doi.org/10.1007/s00253-016-7436-5>

- Kim AD, Graham DE, Seeholzer SH, Markham GD (2000) S-Adenosylmethionine decarboxylase from the archaeon *Methanococcus jannaschii*: identification of a novel family of pyruvoyl enzymes. *J Bacteriol* 182:6667–6672. <https://doi.org/10.1128/JB.182.23.6667-6672.2000>
- Kotelnikova SV, Obratsova AY, Blotvogel KH, Popov IN (1993) Taxonomic analysis of thermophilic strains of the genus *Methanobacterium*: reclassification of *Methanobacterium thermoalcaliphilum* as a synonym of *Methanobacterium thermoautotrophicum*. *Int J Syst Bacteriol* 43:591–596. <https://doi.org/10.1099/00207713-43-3-591>
- Liu Y, Whitman WB (2008) Metabolic, phylogenetic, and ecological diversity of the methanogenic archaea. *Ann N Y Acad Sci* 1125:171–189. <https://doi.org/10.1196/annals.1419.019>
- Lyu Z, Shao N, Akinyemi T, Whitman WB (2018) Methanogenesis. *Curr Biol* 28:R727–R732. <https://doi.org/10.1016/j.cub.2018.05.021>
- Maestrojuan GM, Boone DR, Xun L, Mah RA, Zhang L (1990) Transfer of *Methanogenium bourgense*, *Methanogenium marisnigri*, *Methanogenium olentangyi*, and *Methanogenium thermophilicum* to the genus *Methanoculleus* gen. nov., emendation of *Methanoculleus marisnigri* and *Methanogenium*, and description of new strains of M. *Int J Syst Bacteriol* 40:117–122. <https://doi.org/10.1099/00207713-40-2-117>
- Narihiro T, Kusada H, Yoneda Y, Tamaki H (2016) Draft genome sequences of *Methanoculleus horonobensis* strain JCM 15517, *Methanoculleus thermophilus* strain DSM 2373, and *Methanofollis ethanolicus* strain JCM 15103, hydrogenotrophic methanogens belonging to the family *Methanomicrobiaceae*. *Genome Announc* 4:4–5. <https://doi.org/10.1128/genomeA.00199-16>
- Palù M, Peprah M, Tsapekos P, Kougias P, Campanaro S, Angelidaki I, Treu L (2022) In-situ biogas upgrading assisted by bioaugmentation with hydrogenotrophic methanogens during mesophilic and thermophilic co-digestion. *Bioresour Technol* 348:126754. <https://doi.org/10.1016/j.biortech.2022.126754>
- Pastore LM, Lo Basso G, Quarta MN, de Santoli L (2022) Power-to-gas as an option for improving energy self-consumption in renewable energy communities. *Int J Hydrogen Energy* 47:29604–29621. <https://doi.org/10.1016/j.ijhydene.2022.06.287>
- Rivard CJ, Smith PH (1982) Isolation and characterization of a thermophilic marine methanogenic bacterium, *Methanogenium thermophilicum* sp. nov. *Int J Syst Bacteriol* 32:430–436. <https://doi.org/10.1099/00207713-32-4-430>
- Rotaru AE, Shrestha PM, Liu F, Shrestha M, Shrestha D, Embree M, Zengler K, Wardman C, Nevin KP, Lovley DR (2014) A new model for electron flow during anaerobic digestion: direct interspecies electron transfer to *Methanoseta* for the reduction of carbon dioxide to methane. *Energy Environ Sci* 7:408–415. <https://doi.org/10.1039/c3ee42189a>
- Sunyoto NMS, Zhu M, Zhang Z, Zhang D (2016) Effect of biochar addition on hydrogen and methane production in two-phase anaerobic digestion of aqueous carbohydrates food waste. *Bioresour Technol* 219:29–36. <https://doi.org/10.1016/j.biortech.2016.07.089>
- Szuhaj M, Ács N, Tengölics R, Bodor A, Rákhely G, Kovács KL, Bagi Z (2016) Conversion of H<sub>2</sub> and CO<sub>2</sub> to CH<sub>4</sub> and acetate in fed-batch biogas reactors by mixed biogas community: a novel route for the power-to-gas concept. *Biotechnol Biofuels* 9:1–14. <https://doi.org/10.1186/s13068-016-0515-0>
- Tatusov RL, Natale DA, Garkavtsev IV, Tatusova TA, Shankavaram UT, Rao BS, Kiryutin B, Galperin MY, Fedorova ND, Koonin EV (2001) The COG database: new developments in phylogenetic classification of proteins from complete genomes. *Nucl Acids Res* 29:22–28. <https://doi.org/10.1093/nar/29.1.22>
- Thauer RK (1998) Biochemistry of methanogenesis: a tribute to Marjory Stephenson:1998 Marjory Stephenson Prize Lecture. *Microbiology* 144:2377–2406. <https://doi.org/10.1099/00221287-144-9-2377>
- Vavilin VA, Rytov SV, Lokshina LY (1995) Modelling hydrogen partial pressure change as a result of competition between the butyric and propionic groups of acidogenic bacteria. *Bioresour Technol* 54:171–177. [https://doi.org/10.1016/0960-8524\(95\)00127-1](https://doi.org/10.1016/0960-8524(95)00127-1)
- Wagner T, Watanabe T, Shima S (2018) Hydrogenotrophic methanogenesis. *Biog Hydrocarb* 1–29. [https://doi.org/10.1007/978-3-319-53114-4\\_3-1](https://doi.org/10.1007/978-3-319-53114-4_3-1)
- Yan Q, Ai X, Li J (2021) Low-carbon economic dispatch based on a CCPP-P2G virtual power plant considering carbon trading and green certificates. *Sustain* 13:1–19. <https://doi.org/10.3390/su132212423>
- Zhang G, Wang W, Chen Z, Li R, Niu Y (2022) Modeling and optimal dispatch of a carbon-cycle integrated energy system for low-carbon and economic operation. *Energy* 240:122795. <https://doi.org/10.1016/j.energy.2021.122795>
- Zhao J, Westerholm M, Qiao W, Yin D, Bi S, Jiang M, Dong R (2018) Impact of temperature and substrate concentration on degradation rates of acetate, propionate and hydrogen and their links to microbial community structure. *Bioresour Technol* 256:44–52. <https://doi.org/10.1016/j.biortech.2018.01.150>

**Publisher's note** Springer Nature remains neutral with regard to jurisdictional claims in published maps and institutional affiliations.